TEM study of dislocations structure in $In_{0.82}Ga_{0.18}As$/InP heterostructure with InGaAs as buffer layer[*]

ZHAO Liang (赵亮), GUO Zuo-xing (郭作兴), YUAN De-zeng (袁德增), WEI Qiu-lin (魏秋林), and ZHAO Lei (赵磊)**

Key Lab of Automobile Materials, Ministry of Education, College of Materials Science and Engineering, Jilin University, Changchun 130025, China

In order to improve the quality of detector, $In_xGa_{1-x}As$ ($x=0.82$) buffer layer has been introduced in $In_{0.82}Ga_{0.18}As$/InP heterostructure. Dislocation behavior of the multilayer is analyzed through plane and cross section [110] by transmission electron microscopy (TEM) and high resolution transmission electron microscopy (HRTEM). The dislocations are effectively suppressed in $In_xGa_{1-x}As$ ($x=0.82$) buffer layer, and the density of dislocations in epilayer is reduced obviously. No lattice mismatch between buffer layer and epilayer results in no misfit dislocation (MD). The threading dislocations (TDs) are directly related to the multiplication of the MDs in buffer layer.

Due to the unique properties, the semiconductors of Ⅲ-Ⅴ compounds attract more and more attention in recent years[1-4], which are widely used in microelectronic and optoelectronic fields[5-9]. Particularly, the $In_xGa_{1-x}As$ ($x=0.82$) detectors with the cut-off wavelength of 2.5 μm[10-12] applied in aerospace imaging and spectroscopy attract more interests. To obtain high quality $In_{0.82}Ga_{0.18}As$/InP (100) structures, the lattice defect formation owing to misfit is the chief problem to be solved. Large lattice mismatch of about 2% existing in $In_xGa_{1-x}As$/InP (100) ($x=0.82$) heterostructure brings about amounts of stress in epilayer. The progress of stress relaxation of the heterostructure is usually determined by the formation of dislocations which would further degrade the performance of the detectors[9,13]. In order to restrain the formation of the defects and then obtain high quality detectors, it is very important to classify and analyze the defects in the interface and epilayer. For improving the quality of the detectors, various kinds of buffers have been implemented to reduce the residual strain and decrease the TDs density[14,15]. In our earlier study, the dislocation behavior in $In_xGa_{1-x}As$/InP (100) ($x=0.82$) has been analyzed accurately and directly[16]. In this work, the formation and behavior of dislocations in $In_xGa_{1-x}As$/InP ($x=0.82$) heterostructure with $In_xGa_{1-x}As$ ($x=0.82$) as buffer layer are investigated and analyzed in detail.

The $In_xGa_{1-x}As$/InP (100) ($x=0.82$) heterostructure was grown by low pressure metal organic chemical vapor deposition (LP-MOCVD). The growth was performed using trimethylindium (TMIn), trimethylgallium (TMGa), and 10% arsine (AsH_3) in H_2 as precursors. The palladium-diffused hydrogen was used as carrier gas. The substrates on a graphite susceptor were heated by inductive coupling radio frequency power, the temperature was detected by a thermocouple, the reactor pressure was kept at $1×10^4$ Pa, and the growth temperature was 430 °C with a growth rate of 300 nm/h. Before the growth of the epilayer, the $In_xGa_{1-x}As$ ($x=0.82$) buffer layer was introduced into the structure with the same growth conditions. The microstructure of the interface between the $In_xGa_{1-x}As$/InP (100) ($x=0.82$) heterostructure and the epilayer was detected by transmission electron microscopy (TEM, JEM-2100F, JEOL). High resolution transmission electron microscopy (HRTEM) operating at 200 kV was used for plane and cross section [110] investigation.

Fig.1 shows cross-sectional TEM micrograph of the $In_{0.82}Ga_{0.18}As$/InP heterostructure and plane TEM micrograph of $In_{0.82}Ga_{0.18}As$ epilayer. From Fig.1(a), it can be got that the thicknesses of the buffer layer and epilayer are 201 nm and 1 555 nm, respectively. The dislocation density of the epilayer has been calculated to be $2.143×10^9$ cm^{-2}, which is obviously lower than that of the epilayer without buffer layer reported before[16]. The surface of epilayer can be seen clearly in Fig.1(b). The common dislocation network structure in general epitaxial growth heterostructure has not been found[17-19] in

TEM images. The dislocation density of the epilayer has been calculated to be 1.935×10^9 cm^{-2}.

In order to characterize the dislocations in epilayer deeply, the cross-sectional bright-field images of the $In_{0.82}Ga_{0.18}As$ epilayer obtained with two-beam diffracting conditions using g=1-11, g=11-1 and g=220 (g is the reflection when taking the TEM photo) are shown in Fig.2. Dislocation group A is invisible in Fig.2(a) and (c), which shows obvious contrast in Fig.2(b). Based on extinction condition of $g \cdot b$=0 (b is the Burgers vector), the Burgers vector of dislocation group A can be given as b=a/2[110] (a is the crystal constant). Dislocation group C is invisible in Fig.2(a), showing residual contrast in Fig.2(c) while obvious contrast in Fig.2(b). The Burgers vector of dislocation group C can be given as b=a/2[110]. Dislocation groups B and D show non-contrast in Fig.2(a) and (b) while obvious contrast in Fig.2(c). The Burgers vector of dislocation groups B and D can be given as b=a/2[011].
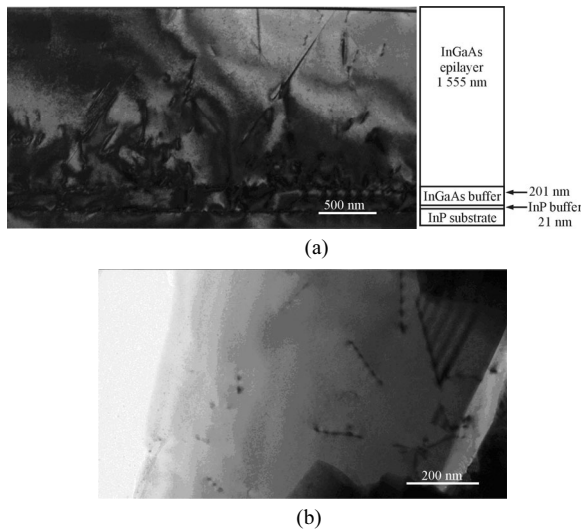

(a)

(b)

Fig.1 (a) Cross-sectional bright-field image of the $In_{0.82}Ga_{0.18}As$/InP heterostructure using g=1-11 and (b) plane-view bright-field image of the $In_{0.82}Ga_{0.18}As$ epilayer using g=200 obtained with two-beam diffracting conditions

In order to analyze the structure of the interface in detail, HRTEM images of the interface between substrate and buffer layer and the interface between buffer layer and epilayer have been detected and shown in Fig.3(a)—(g). Fig.3(a) shows the HRTEM image of the interface between the substrate and buffer layer. The fast Fourier transform (FFT) images of substrate and buffer layer regions are shown in Fig.3(b) and (c). Based on the two images, the crystal constants of substrate and buffer layer are calculated to be a=0.586 6 nm and a=0.609 1 nm, respectively. The results are in good accordance with the crystal constant calculated using the doping amount: a=0.609 1 nm. Fig.3(d) shows the inverse fast Fourier transform (IFFT) HRTEM image of the interface. From it, a lot of misfit dislocations (MDs) can be realized, and more of them are 60° disloca-

tions. In the interface between the buffer layer and epilayer, a lot of stacking faults and dislocations can be detected, as shown in Fig.3(e)—(g). Most of these dislocations are 60° and 90° dislocations. The results are in good agreement with previous studies[16].
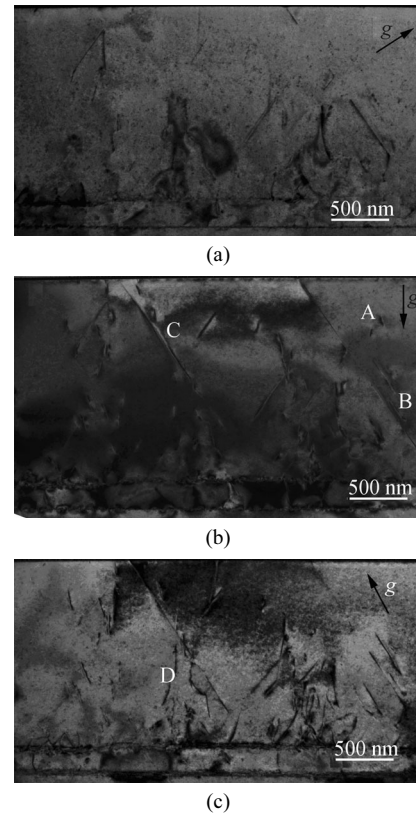

(a)

(b)

(c)

Fig.2 Cross-sectional TEM images of the $In_{0.82}Ga_{0.18}As$/InP heterostructure for (a) g=1-11, (b) g=11-1 and (c) g=220
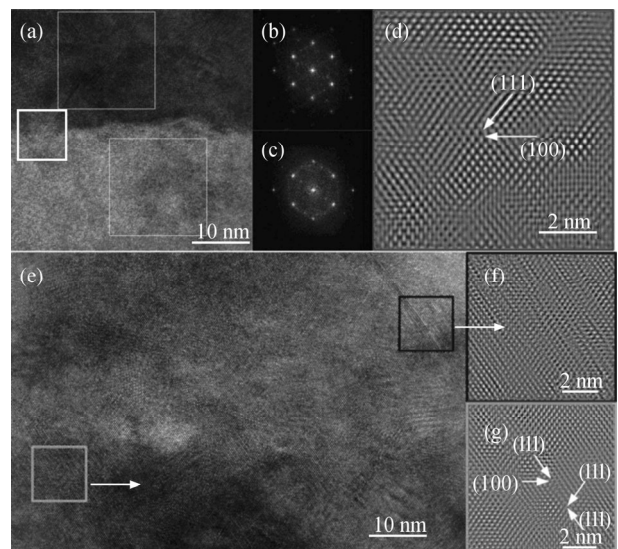

Fig.3 (a) HRTEM image of the interface between substrate and buffer layer; (b, c) FFT images of different regions in (a); (d) IFFT HRTEM image of the interface; (e) HRTEM image of the interface between buffer layer and epilayer; (f, g) IFFT HRTEM images of different regions in (e)

In order to further verify the effect of buffer layer on reducing the dislocation density, the HRTEM images of different regions have been taken and shown in Fig.4(a)—(e). According to these images, the dislocation densities of different regions are calculated. The highest dislocation density of 7.4×10^{12} cm^{-2} is got in buffer layer, and the lowest dislocation density of 2×10^{11} cm^{-2} is got in epilayer. This proves that the buffer layer can greatly block the movement of dislocations and significantly reduce the dislocation density in the epilayer.
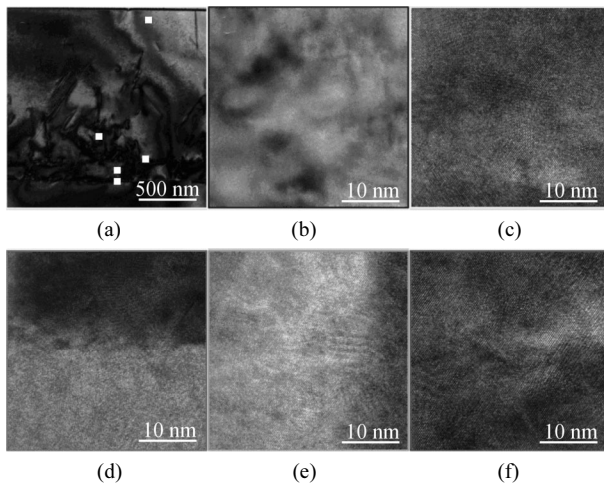

Fig.4 (a) Cross-sectional TEM image of the In$_{0.82}$Ga$_{0.18}$As/InP heterostructure; HRTEM images of different regions of the sample: (b) Near the surface of epilayer; (c) Near the interface between epilayer and buffer layer; (d) The interface between epilayer and buffer layer; (e) The buffer layer; (f) The interface between buffer layer and substrate

In order to improve the quality of detector, the In$_x$Ga$_{1-x}$As (x=0.82) buffer layer has been introduced in In$_{0.82}$Ga$_{0.18}$As/InP heterostructure. The dislocations are effectively suppressed in In$_x$Ga$_{1-x}$As (x=0.82) buffer layer, and the dislocation density of epilayer is obviously reduced. No lattice mismatch between buffer layer and epilayer results in no MD. Therefore, the threading dislocations (TDs) are directly related to the multiplication of the MDs in buffer layer.

References

[1]   F. Zheng, G. Zhu, X.F. Liu, C. Wang, Z.B. Sun and G.J. Zhai, Optoelectronics Letters **11**, 121 (2015).

[2]   L. Avakyants, P.Y. Bokov, T. Kolmakova and A. Chervyako, Semiconductors **38**, 1384 (2004).

[3]   X. Jin, H. Nakahara, K. Saitoh, T. Saka, T. Ujihara, N. Tanaka and Y. Takeda, Journal of Crystal Growth **353**, 84 (2012).

[4]   L.S. Liu, Optoelectronics Letters **6**, 191 (2010).

[5]   J.F. Geisz, S. Kurtz, M.W. Wanlass, J.S. Ward, A. Duda, D.J. Friedman, J.M. Olson, W.E. McMahon, T.E. Moriarty and J.T. Kiehl, Applied Physics Letters **91**, 023502 (2007).

[6]   L. Avakyants, P.Y. Bokov, G. Galiev, V. Kaminskii, V. Kul'bachinskii, V. Mokerov and A. Chervyakov, Optics and Spectroscopy **93**, 857 (2002).

[7]   M. Hostut, M. Alyoruk, T. Tansel, A. Kilic, R. Turan, A. Aydinli and Y. Ergun, Superlattices and Microstructures **79**, 116 (2015).

[8]   N. Tounsi, M.M. Habchi, Z. Chine, A. Rebey and B. El Jani, Superlattices and Microstructures **59**, 133 (2013).

[9]   T. Zhang, G. Miao, Y. Jin, H. Jiang, Z. Li and H. Song, Journal of Alloys and Compounds **458**, 363 (2008).

[10]   K. Oe, Journal of Crystal Growth **219**, 10 (2000).

[11]   S. Wang, W. Wang, H. Zhu, L. Zhao, R. Zhang, F. Zhou, H. Shu and R. Wang, Journal of Crystal Growth **260**, 464 (2004).

[12]   Y. Zhu, H.Q. Ni, H.L. Wang, J.F. He, M.F. Li, X.J. Shang and Z.C. Niu, Optoelectronics Letters **7**, 325 (2011).

[13]   S.K. Mathis, P. Chavarkar, A.M. Andrews, U.K. Mishra and J.S. Speck, Journal of Vacuum Science & Technology B: Microelectronics and Nanometer Structures **18**, 2066 (2000).

[14]   M. Gutiérrez, D. González, G. Aragón, M. Hopkinson and R. García, Materials Science and Engineering: B **80**, 27 (2001).

[15]   L.J. Mawst, J.D. Kirch, C.C. Chang, T. Kim, T. Garrod and D. Botez, Journal of Crystal Growth **370**, 230 (2013).

[16]   L. Zhao, J.G. Sun, Z.X. Guo and G.Q. Miao, Materials Letters **106**, 222 (2013).

[17]   L.H. Wong, J.P. Liu, F. Romanato, C.C. Wong and Y.L. Foo, Applied Physics Letters **90**, 061913 (2007).

[18]   T. Wosiński, T. Figielski, A. Mąkosa, W. Dobrowolski, O. Pelya and B. Pécz, Materials Science and Engineering: B **91**, 367 (2002).

[19]   J. Kim, E. Yun, J. Yu, K. Park, S. Chai, J. Yang and S. Choi, Materials Letters **53**, 446 (2002).